Int. J. Morphol.,
44(4):1500-1508, 2026.

Endoscopic Transoral Approach to the Parapharyngeal Space: A Cadaveric Anatomical Study with Single Clinical Case Validation

Abordaje Endoscópico Transoral al Espacio Parafaríngeo: Estudio Anatómico en Cadáveres con Validación Mediante un Caso Clínico Único

The Viet Tran[1]; Quang Tuyen Le[2] & Huyen Tran Lam[2]

TRAN, T. V.; LE, Q. T. & LAM, H. T. Endoscopic transoral approach to the parapharyngeal space: A cadaveric anatomical study with single clinical case validation. *Int. J. Morphol., 44(4)*:1500-1508, 2026.

SUMMARY: The parapharyngeal space (PPS) is a deep cervical space whose intimate relationship with the internal carotid artery (ICA) and lower cranial nerves makes surgery within it technically demanding. The endoscopic transoral approach (ETA) offers a minimally invasive alternative to classical open routes; however, systematic quantitative descriptions of the inside-out anatomy visible through this corridor remain scarce. The objective of this study was twofold: (1) to describe the layered anatomy of the PPS as encountered during endoscopic transoral dissection in fresh cadaveric specimens, with measurement of ICA distances from two clinically relevant landmarks; and (2) to validate the translational applicability of these cadaveric findings through a single clinical case. Endoscopic transoral dissection was performed on 10 fresh adult cadaveric specimens (20 sides) using rigid 0° and 30° endoscopes following carotid injection with colored contrast. Two bilateral measurements were recorded with 1-mm precision: pterygoid hamulus-to-ICA (PTH-ICA) and pharyngeal mucosa-to-ICA (Mucosa-ICA) distances. One patient with a prestyloid PPS tumor meeting cadaveric-defined anatomical criteria subsequently underwent ETA. Stepwise dissection consistently identified the pharyngeal mucosa, superior pharyngeal constrictor, prestyloid fat compartment, styloglossus and stylopharyngeus muscles, styloid diaphragm, and stylohyoid ligament before reaching the ICA. Mean PTH-ICA distance was 26.36 ± 2.94 mm (left) and 27.15 ± 5.11 mm (right); mean Mucosa-ICA was 22.85 ± 2.79 mm (left) and 23.04 ± 2.42 mm (right). No significant left-right asymmetry was detected ($p > 0.05$). In the clinical case, operative time was 45 min, blood loss < 50 mL, with no intraoperative complications; histopathology confirmed pleomorphic adenoma with no recurrence at six months. The cadaveric study defines a reproducible layered anatomical corridor for ETA, with the pterygoid hamulus and stylopharyngeus muscle as key safety landmarks. The clinical case confirms direct translation of cadaveric findings to operative practice, supporting the safety and feasibility of ETA for small-to-medium benign prestyloid PPS tumors.

KEY WORDS: Parapharyngeal space; Endoscopic transoral approach; Surgical anatomy; Cadaveric study; Pleomorphic adenoma.

INTRODUCTION

The parapharyngeal space (PPS) is a deep cervical space with an inverted pyramidal shape, extending from the skull base superiorly to the hyoid bone inferiorly. It is bounded medially by the superior pharyngeal constrictor, laterally by the ramus of the mandible, anteriorly by the pterygomandibular raphe, and posteriorly by the prevertebral muscles (Curtin, 1987; Olsen, 1994). The tensor-vascular-styloid (TVS) fascia divides the PPS into a prestyloid compartment—containing predominantly adipose tissue and the deep lobe of the parotid gland—and a poststyloid compartment housing the ICA, internal jugular vein, and cranial nerves IX–XII (Riffat *et al*., 2014). A spectrum of pathological conditions may arise within or secondarily involve this space, necessitating surgical intervention. Primary PPS neoplasms include benign tumors—predominantly pleomorphic adenoma and other salivary gland tumors of parotid deep-lobe or minor salivary gland origin, paragangliomas (carotid body tumors, vagal paragangliomas, jugulotympanic tumors), schwannomas and neurofibromas of cranial nerves IX–XII, and lipomas—as well as malignant tumors such as carcinoma ex pleomorphic adenoma, mucoepidermoid carcinoma, and primary lymphoma. Secondary involvement occurs through direct extension from adjacent spaces (masticator, retropharyngeal, parotid) in the setting of locally advanced head and neck carcinoma, or through nodal metastatic

[1] Department of Otorhinolaryngology, School of Medicine, University of Medicine and Pharmacy at Ho Chi Minh City (UMP), Ho Chi Minh City, Vietnam.
[2] Department of Anatomy, Pham Ngoc Thach University of Medicine, Ho Chi Minh City, Vietnam.

Received: 2026-04-24 Accepted: 2026-06-25

disease. Non-neoplastic conditions requiring surgery include deep neck space abscesses with parapharyngeal extension, vascular anomalies such as aberrant ICA or pseudoaneurysm, and styloid process elongation (Eagle syndrome) causing neurovascular compression (Olsen, 1994; Riffat *et al*., 2014). Because of its deep location and intimate relationship with critical neurovascular structures, surgery within this space represents one of the greatest challenges in head and neck surgery.

Classical surgical approaches to the PPS include the transcervical, transparotid, transmandibular, and combined cervico-transoral routes (Paderno *et al*., 2015; Lombardi *et al*., 2020). While effective for larger or vascularized lesions, these approaches carry inherent limitations including external scarring, risk of facial nerve injury, and prolonged recovery. In this context, the endoscopic transoral approach (ETA) has emerged as a minimally invasive alternative that allows direct access to the PPS without external incision, while leveraging endoscopic magnification to visualize deep anatomical structures (Chan *et al*., 2011; Dallan *et al*., 2011).

Although ETA for PPS lesions has been reported sporadically, concerns persist regarding safety—particularly the risk of injury to the ICA and lower cranial nerves (Boyce *et al*., 2016; Li *et al*., 2020). The ETA also carries inherent technical limitations that must be recognized: access is restricted to small-to-medium lesions (generally < 4 cm), and tumors with significant superior extension toward the skull base, posterior extension into the retrostyloid compartment, or those with evidence of vascular encasement or malignant infiltration are not suitable candidates. Furthermore, the transoral working corridor provides limited maneuverability for standard two-handed dissection, requires familiarity with endoscopic orientation in a narrow, non-expanded field, and carries a risk of incomplete tumor removal if capsular rupture occurs in the deep confined space. Postoperative oropharyngeal swelling and the potential for deep-space hematoma are also specific concerns with this approach. A fundamental challenge compounding these limitations is the limited availability of systematic, quantitative descriptions of the inside-out anatomy of the PPS as seen through the transoral endoscopic perspective (Gun *et al*., 2016). Such reference data are necessary for procedural standardization and for translating cadaveric findings into consistent clinical practice.

This study was designed with two explicitly linked objectives: (1) to systematically describe the anatomical layers of the PPS encountered during endoscopic transoral dissection in 10 fresh cadaveric specimens, with quantitative measurement of ICA distances from two clinically relevant landmarks; and (2) to validate the clinical applicability of these findings through a single illustrative case of a prestyloid PPS tumor successfully resected by ETA using the dissection protocol derived from the cadaveric phase.

MATERIAL AND METHOD

Study Design

This study used an integrated two-phase design: a primary descriptive cadaveric anatomical investigation followed by a single clinical application case. The cadaveric phase established the stepwise anatomical roadmap and quantitative reference data for ETA; the clinical phase prospectively applied this protocol in one patient meeting the anatomical selection criteria defined by the cadaveric study.

Cadaveric Study

Specimens. Ten fresh adult cadaveric specimens (20 sides) were used. All specimens were free of prior head and neck surgery, congenital anomalies, or anatomical abnormalities of the pharyngeal-cervical region. Specimens were refrigerated and the carotid arteries were injected with colored contrast medium prior to endoscopic transoral dissection. The use of human cadaveric material is acknowledged in accordance with the recommendations of Iwanaga *et al*. (2021).

Positioning and instrumentation. Cadavers were placed in a supine position with the head gently extended and the mouth maximally opened with a standard mouth gag. Open bilateral neck dissection was performed prior to endoscopic dissection to expose the carotid bundles and facilitate carotid injection. Dissection was performed using rigid 0° and 30° endoscopes (4 mm diameter), a cold light source, and a high-definition camera system.

Endoscopic transoral dissection protocol. A standardized stepwise protocol was followed: (1) exposure of the lateral pharyngeal wall and identification of the palatine tonsillar fossa; (2) incision of the pharyngeal mucosa along the anterior tonsillar pillar with submucosal dissection; (3) identification and incision of the superior pharyngeal constrictor parallel to its fiber orientation (i.e., in a fiber-splitting rather than transverse manner) to minimize muscular disruption; (4) exposure of the prestyloid fat compartment; and (5) careful dissection to identify the styloid muscles (styloglossus and stylopharyngeus) and locate the ICA through the styloid diaphragm. The pterygoid hamulus, levator veli palatini, styloid muscles, and carotid bundle were systematically recorded as anatomical landmarks.

Anatomical measurements. Bilateral measurements were performed with a surgical ruler (1-mm accuracy): (1) distance from the pterygoid hamulus to the medial margin of the ICA (PTH-ICA); and (2) distance from the pharyngeal mucosa at the anterior tonsillar pillar insertion to the ICA (Mucosa-ICA). Each measurement was performed twice by the same surgeon and the mean value used for analysis.

Statistical analysis

Data are presented as mean ± SD with 95 % confidence intervals (CI) and range. Normality was assessed by the Shapiro-Wilk test. Comparison between sides used paired t-tests or Wilcoxon signed-rank test as appropriate; comparison between the two landmark types used an independent samples t-test. Left-right correlation was assessed by Pearson's coefficient. A p-value < 0.05 was considered statistically significant. All analyses were performed using Python 3 (scipy.stats library).

Single Clinical Case

Patient selection. One patient with a diagnosed prestyloid PPS lesion was enrolled. Inclusion criteria—defined based on cadaveric findings—were: benign prestyloid location, maximum diameter < 4 cm, well-circumscribed margins on MRI, and no evidence of vascular invasion or ICA displacement. Diagnosis was established on clinical findings and MRI imaging. Written informed consent was obtained prior to participation.

Surgical procedure. Surgery was performed under general anesthesia with orotracheal intubation, following the ETA protocol established through the cadaveric study. Landmark orientation used the pterygoid hamulus and stylopharyngeus muscle as primary ICA safety references. Operative time, estimated blood loss, and intraoperative complications were recorded.

Postoperative follow-up. Postoperative monitoring included assessment of swallowing function, hemorrhage, lower cranial nerve function, and infectious complications. Histopathological analysis was performed on the resected specimen.

Ethical Considerations

This study was conducted in compliance with biomedical research ethics principles (approval decision no. 25273-DHYD, signed June 4, 2025) and in accordance with the principles of the Declaration of Helsinki. Cadaveric dissection was performed in accordance with institutional regulations governing anatomical research. The patient included in the clinical case provided full written informed consent prior to participation.

RESULTS

Cadaveric Study

Endoscopic transoral dissection was performed on 10 fresh cadaveric specimens (20 sides), systematically exposing the anatomical layers of the PPS from an inside-out perspective.

Pharyngeal mucosa. The innermost layer encountered is the mucosa covering the medial surface of the lateral pharyngeal wall, enveloping the palatine tonsillar fossa and the palatine arches. Incision through the pharyngeal mucosa reveals the underlying muscular layer, facilitating orientation toward the PPS (Fig. 1a).

Superior pharyngeal constrictor muscle. Immediately deep into the mucosa lies the superior pharyngeal constrictor, forming the lateral pharyngeal wall. An incision parallel to the fiber orientation of this muscle (fiber-splitting approach) creates a window into the PPS (Fig. 1b).

Prestyloid fat compartment. Immediately lateral to the superior pharyngeal constrictor, the prestyloid compartment consists predominantly of loose adipose tissue. This fat pad serves as a natural safety buffer between the pharyngeal wall and the major neurovascular structures and also contains the deep lobe of the parotid gland, ascending palatine and pharyngeal arterial branches, and tributaries and extensions of the pterygoid venous plexus (the main plexus itself being situated in the infratemporal fossa, lateral to the lateral pterygoid muscle). Prestyloid PPS tumors typically arise within this compartment and displace adjacent structures posteriorly as they enlarge (Riva *et al*., 2022).

Styloglossus muscle. Deeper dissection encounters the styloglossus muscle. From an endoscopic transoral (inside-out) perspective, the muscle is observed traveling from a lateral and deep origin (the styloid process) toward a medial and superficial insertion (the lateral tongue), so that its trajectory within the endoscopic field appears to run from lateral/deep to medial/superficial. This endoscopic orientation—distinct from the classical anatomical description of a posterosuperior-to-anteroinferior trajectory—serves as a practical navigational guide: the surgeon should dissect medial and anterior to the styloglossus to remain in the prestyloid compartment and away from the posterior neurovascular structures. In all 10 dissected specimens, the styloglossus was consistently present with a stable course, serving as a reliable orientation

guide and protective layer for the posterior vascular structures (Laccourreye *et al*., 2018).

Stylopharyngeus muscle. At the level of the styloid diaphragm, the stylopharyngeus muscle appears as a longitudinal muscular band descending along the outer surface of the pharyngeal wall. The ascending palatine artery ascends between the styloglossus and stylopharyngeus; the glossopharyngeal nerve (CN IX) descends along the posterior margin of the stylopharyngeus. Together, the styloglossus and stylopharyngeus form the anterior landmark of the juxtapharyngeal segment of the ICA (Gun *et al*., 2016). Critically, in the context of ETA, the stylopharyngeus must be regarded as the functional last line of defense before the ICA: once the surgeon has passed the stylopharyngeus posteriorly, the retrostyloid neurovascular bundle—and particularly the ICA—is immediately at risk. Dissection should therefore always respect the stylopharyngeus as the definitive posterior boundary of safe prestyloid dissection.

Styloid diaphragm (stylopharyngeal fascia). Overlying the styloid muscular group is the styloid diaphragm—a composite muscular-fascial unit comprising the styloid muscles (styloglossus, stylopharyngeus, stylohyoid) and their investing fascia—which forms a partition between the prestyloid and retrostyloid PPS compartments. The tensor-vascular-styloid (TVS) fascia is the specific dense connective tissue component within this unit, extending from the styloid process to the skull base (Riffat *et al*., 2014); it should not be used as a synonym for the entire styloid diaphragm, which additionally encompasses the muscular elements. This muscular-fascial complex encases the styloid muscles, separates the prestyloid fat from the neurovascular bundle, and provides a protective barrier anteriorly covering the ICA (Fig. 1c). For prestyloid lesions, the styloid diaphragm should be deliberately preserved as a protective shield; it should only be intentionally opened when pathology extends into or originates from the poststyloid (retrostyloid) compartment.

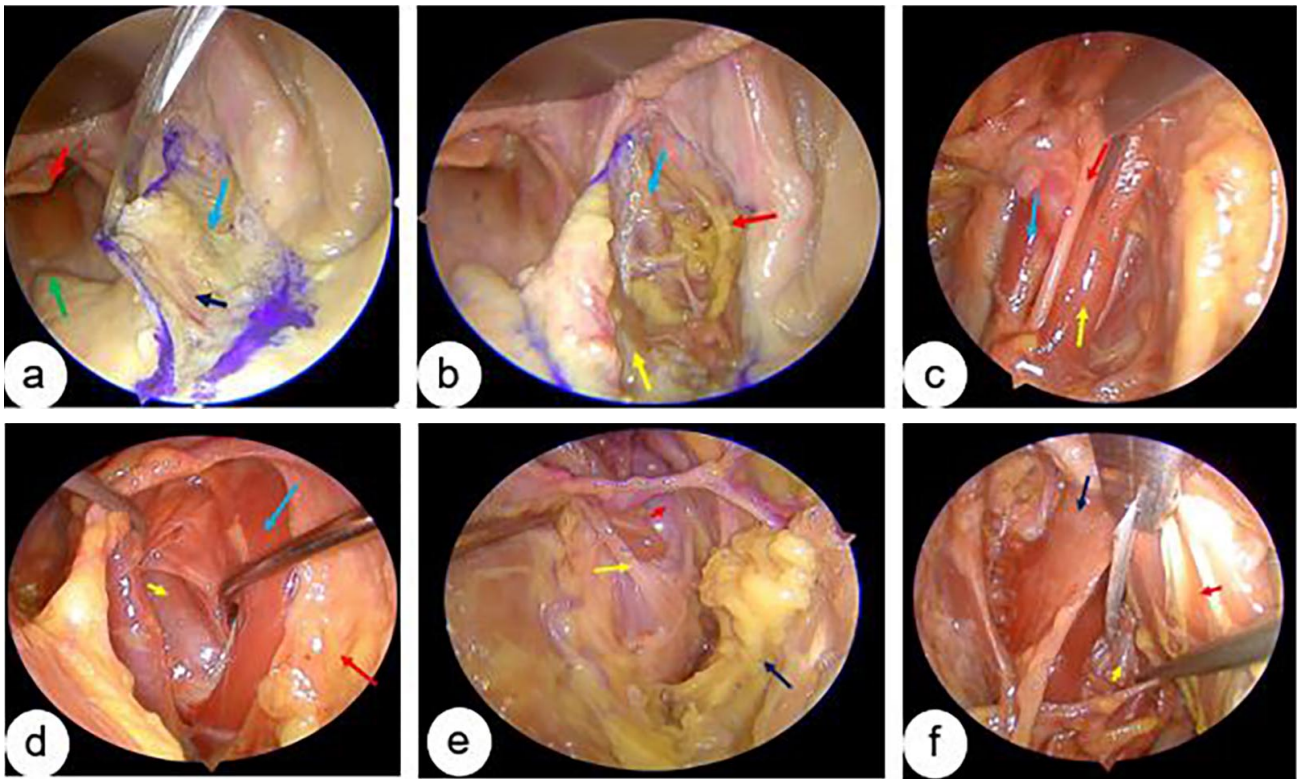


Fig. 1. Incision through the pharyngeal mucosa. **(a)** After incising the pharyngeal mucosa, minor salivary gland tissues, and the overlying fascia, the fat layer of the parapharyngeal space (PPS) is exposed. Red arrow indicates epiglottis, blue arrow indicates parapharyngeal fat pad, dark blue arrow indicates superior pharyngeal constrictor muscle. **(b)** The prestyloid compartment of the PPS is exposed following incision of the superior pharyngeal constrictor. Blue arrow indicates styloglossus muscle, red arrow indicates parapharyngeal space fat and yellow arrow indicates superior pharyngeal constrictor muscle. **(c)** The styloid diaphragm, bounded by the styloglossus muscle (yellow arrow), stylohyoid muscle (blue arrow), and stylohyoid ligament (red arrow). **(d)** The internal carotid artery (ICA, yellow arrow) is exposed after retracting the stylopharyngeus muscle (blue arrow) while red arrow indicates parapharyngeal fat pad. **(e)** The glossopharyngeal nerve (CN IX, yellow arrow) is exposed, crossing over the internal carotid artery (red arrow) and dark blue arrow indicates parapharyngeal fat pad. **(f)** Measurement of the distance from the pterygoid hamulus to the internal carotid artery. Dark blue arrow indicates pterygoid hamulus, red arrow indicates medial pterygoid muscle, and yellow arrow indicates internal carotid artery.

Stylohyoid ligament. The stylohyoid ligament appears as a firm white fibrous band running from the styloid process toward the lesser horn of the hyoid bone, constituting one of the anterior landmarks of the juxtapharyngeal ICA segment.

Carotid bundle (retrostyloid compartment). The ICA and internal jugular vein, along with cranial nerves IX–XII, are contained within the retrostyloid compartment protected anteriorly by the styloid diaphragm. In all specimens, the ICA was identifiable through a thin fascial layer under endoscopic visualization after dissection through the styloid diaphragm (Fig. 1d).

ICA identification through ETA. Following identification of the styloglossus and stylopharyngeus muscles, the ICA could be reliably identified under endoscopic guidance in all specimens. The ICA lies posterior to the stylopharyngeus muscle, parallel and adjacent to the lateral margin of the prevertebral musculature, in a sagittal plane passing through the pterygoid hamulus. Key landmarks for safe orientation included: (1) the pterygoid hamulus, which consistently lies in the same sagittal plane as the ICA; and (2) the stylopharyngeus muscle, which marks the anterior boundary of the juxtapharyngeal ICA (Figs. 1e, 1f).

Anatomical Measurements

Quantitative anatomical measurements are summarized in Table I.

PTH-ICA *vs.* Mucosa-ICA comparison. The pterygoid hamulus landmark was significantly farther from the ICA than the pharyngeal mucosal surface (independent t-test: $t = 3.545$, $p = 0.001$), with a mean difference of approximately 3.8 mm (26.75 vs. 22.95 mm pooled).

Left-right symmetry. No significant difference was detected between sides for either measurement (PTH-ICA: Wilcoxon $p = 1.000$; Mucosa-ICA: paired t-test $p = 0.503$). High left-right correlation was observed (PTH-ICA: $r = 0.809$, $p = 0.005$; Mucosa-ICA: $r = 0.955$, $p < 0.001$), confirming bilateral anatomical symmetry.

Normality. Three of four measurement groups passed the Shapiro-Wilk test ($p > 0.05$). The PTH-ICA Right group deviated from normality ($W = 0.838$, $p = 0.042$), attributed to a single outlier value (specimen 3: 39.7 mm), with non-parametric Wilcoxon testing applied accordingly.

Single Clinical Case

A 65-year-old female patient was incidentally found to have a left prestyloid PPS mass measuring approximately 3.2×2.5 cm on MRI. The lesion demonstrated well-defined margins, homogeneous signal intensity, and no vascular invasion—meeting the anatomical safety criteria for ETA (diameter < 4 cm, well-circumscribed, non-vascular, ICA protected by intact styloid diaphragm). Imaging findings were consistent with a minor salivary gland tumor of the prestyloid PPS (Li *et al*., 2025) (Fig. 2a).

Surgery was performed under general anesthesia via the ETA protocol derived from the cadaveric study. The sequential dissection steps followed the cadaveric roadmap: incision of the lateral pharyngeal wall mucosa, dissection through the superior pharyngeal constrictor using a fiber-splitting approach, entry into the prestyloid fat compartment, and careful dissection anterior to the stylopharyngeus muscle. The styloid diaphragm was identified and preserved intact as the definitive posterior safety boundary; as this was a prestyloid lesion, deliberate opening of the diaphragm was neither required nor performed, in keeping with the principle that the diaphragm should only be intentionally breached for poststyloid pathology. Landmark orientation using the pterygoid hamulus (~27 mm anterior-lateral to the ICA) and the stylopharyngeus muscle as the anterior ICA boundary maintained a safe dissection corridor throughout. No external incision was required. Operative time was 45 minutes. Estimated blood loss was < 50 mL. No intraoperative complications were recorded (Figs. 2b, 2c, 2d).

Table I. Anatomical measurements of the parapharyngeal space from endoscopic transoral dissection (10 cadaveric specimens, 20 sides).

Measurement	Mean ± SD	95% CI (mm)	Range (mm)
PTH-ICA Left	26.36 ± 2.94	24.26–28.46	21.4–30.1
PTH-ICA Right	27.15 ± 5.11	23.49–30.81	21.9–39.7
Mucosa-ICA Left	22.85 ± 2.79	20.86–24.84	19.7–26.6
Mucosa-ICA Right	23.04 ± 2.42	21.31–24.77	19.1–25.6

ICA: internal carotid artery; PTH: pterygoid hamulus; Mucosa: pharyngeal mucosa at anterior tonsillar pillar; SD: standard deviation; CI: confidence interval.

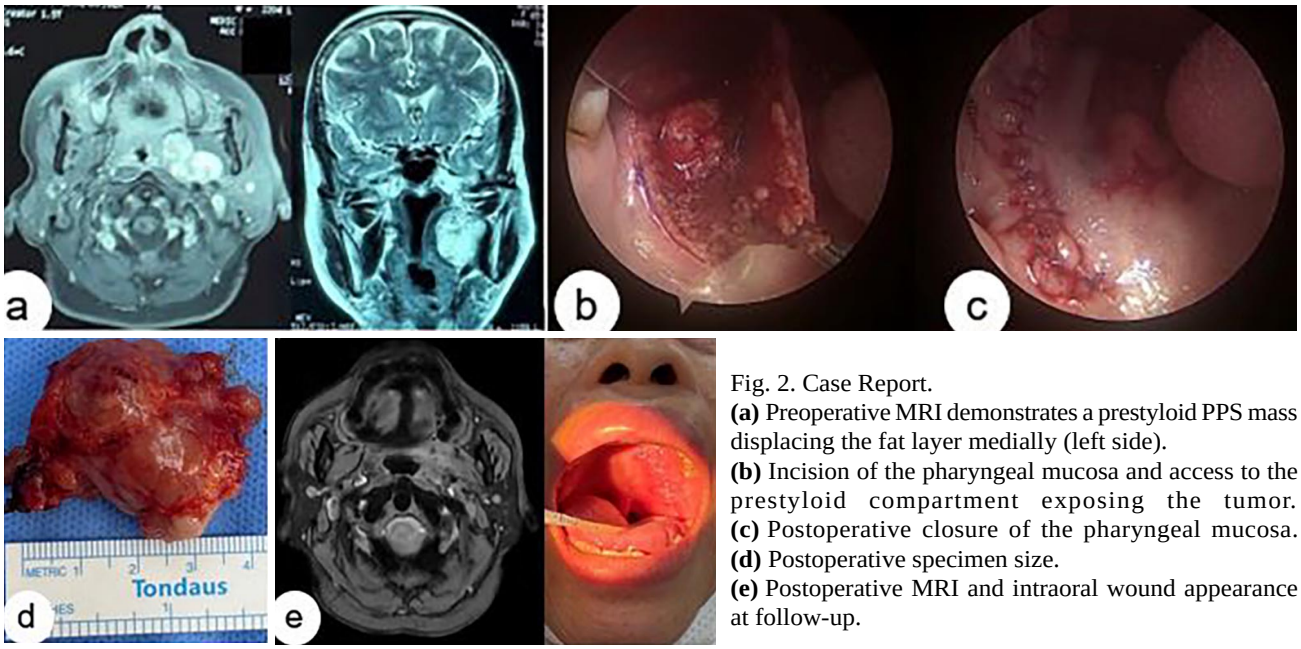


Fig. 2. Case Report.
(a) Preoperative MRI demonstrates a prestyloid PPS mass displacing the fat layer medially (left side).
(b) Incision of the pharyngeal mucosa and access to the prestyloid compartment exposing the tumor.
(c) Postoperative closure of the pharyngeal mucosa.
(d) Postoperative specimen size.
(e) Postoperative MRI and intraoral wound appearance at follow-up.

The patient recovered uneventfully; oral intake resumed at 48 hours postoperatively. No hemorrhagic, neurological, or infectious complications were observed. The patient was discharged on postoperative day five. Histopathological examination confirmed pleomorphic adenoma. No recurrence was noted at six-month follow-up (Fig. 2e).

DISCUSSION

Surgical Access to the PPS

Surgery of the PPS remains one of the most demanding procedures in head and neck surgery, due to its deep location, narrow confines, and close proximity to major vascular and neural structures (Curtin, 1987; Lombardi *et al*., 2020). Conventional open approaches—transcervical, transparotid, and transmandibular routes—while providing adequate exposure are associated with a well-documented spectrum of complications and long-term disabilities. These include permanent facial nerve paresis or paralysis (transparotid approach), Frey syndrome and aesthetic parotid hollowing, Horner syndrome from sympathetic chain injury, lower cranial nerve palsies (dysphagia from CN IX/X injury, shoulder weakness from CN XI, tongue deviation from CN XII), visible neck or submandibular scars, trismus following transmandibular osteotomy, prolonged hospital stay, and a non-negligible rate of perioperative hemorrhage requiring re-exploration (Paderno *et al*., 2015; Lombardi *et al*., 2020). For patients who develop permanent lower cranial nerve dysfunction, the functional consequences—including chronic aspiration, dysphagia, and dysarthria—may persist as lifelong disabilities affecting quality of life. With advances in endoscopic technology, the ETA has gained recognition as a viable alternative for selected PPS lesions, directly addressing many of these limitations: it avoids external incision and its associated cosmetic morbidity, eliminates the risk of facial nerve injury inherent to transparotid dissection, provides direct visualization of deep anatomical structures through endoscopic magnification, and is associated with shorter operative times and earlier functional recovery in reported series (Dallan *et al*., 2011; Paderno *et al*., 2015; Li *et al*., 2025). Our cadaveric study provides a systematic description of the inside-out layered anatomy of the PPS as encountered through the transoral endoscopic corridor, with the aim of supporting safer adoption of this approach.

The sequential layers identified—pharyngeal mucosa, superior pharyngeal constrictor, prestyloid fat compartment, styloglossus, stylopharyngeus, styloid diaphragm, and the retrostyloid neurovascular bundle—constitute a reproducible anatomical roadmap, consistent with previously published transoral cadaveric descriptions (Dallan *et al*., 2011; Gun *et al*., 2016). Critically, the styloid diaphragm serves as a key protective barrier for the ICA, meaning that inadvertent injury to this vessel is unlikely if the surgeon remains within the prestyloid plane. This finding has direct implications for operative safety and supports a stepwise, layer-by-layer dissection strategy.

Anatomical Landmarks for Safe ETA

Two landmarks emerge as particularly important for safe ETA dissection: (1) the pterygoid hamulus as a reliable anterior-lateral fixed bony reference point for ICA localization (mean PTH-ICA distance: 26.75 mm), and (2) the stylopharyngeus muscle as the anterior boundary marker for the juxtapharyngeal ICA. It should be emphasized that, from a transoral endoscopic perspective, the pterygoid hamulus lies anterior and lateral to the ICA—not superior to it; the term "superior" is anatomically misleading given that the hamulus is positioned considerably inferior to the skull base where the ICA enters the carotid canal. Its value as a landmark lies in its role as a fixed anterior-lateral bony anchor that orients the surgeon's depth of dissection in the sagittal plane, as the ICA consistently projects in a sagittal plane passing through the hamulus. These observations are consistent with published transoral anatomical descriptions (Dallan *et al*., 2011; Gun *et al*., 2016; Laccourreye *et al*., 2018) and with the radiological data of Paderno *et al*. (2015), who reported comparable ICA-surface distances via endonasal approaches.

Of note, the pharyngeal mucosal surface was consistently closer to the ICA (~23 mm) than the pterygoid hamulus (~27 mm), a difference that was statistically significant ($p = 0.001$). While this might suggest that the mucosal surface could serve as a navigation reference, an important practical caveat must be recognized: pharyngeal mucosa is a highly mobile and deformable tissue whose position changes substantially depending on the degree of mouth-gag retraction, tissue edema, and intraoperative tension. This mobility introduces measurement variability that limits its reliability as an intraoperative depth reference. In contrast, the pterygoid hamulus is a fixed bony landmark unaffected by soft-tissue deformation or retraction, making it fundamentally more reliable for consistent intraoperative navigation. The appropriate clinical interpretation is therefore that the PTH provides a stable anterior-lateral anchor for orientation, while the ~23 mm mucosal-ICA distance serves as a supplementary depth estimate to be applied cautiously given mucosal mobility. High bilateral symmetry (Mucosa-ICA: $r = 0.955$, $p < 0.001$) supports using either side as an equivalent anatomical reference.

Clinical Translation: From Cadaveric Protocol to Operative Practice

A central strength of this study is its translational design: the clinical case was specifically chosen to reflect the prestyloid anatomical scenario studied in the cadaveric phase. The patient's tumor characteristics—prestyloid location, diameter < 4 cm, well-circumscribed margins, no ICA involvement—matched exactly the anatomical profile for which the cadaveric measurements predict a safe ICA margin of approximately 23–27 mm. The favorable operative outcome—no complications, 45-minute operative time, < 50 mL blood loss, discharge on postoperative day five, histopathologically confirmed pleomorphic adenoma, and no recurrence at six months—directly validates the clinical utility of the cadaveric reference data. These results are consistent with published series reporting ETA for comparable prestyloid PPS lesions (Boyce *et al*., 2016; Li *et al*., 2020; Borello *et al*., 2024).

The inclusion of a clinical case alongside cadaveric data follows an established methodological tradition in surgical anatomy (Dallan *et al*., 2011; Sun *et al*., 2018). Cadaveric studies in isolation carry an inherent translational gap: they describe what can be seen, but do not confirm that the anatomical knowledge translates to safe surgery. A single well-documented clinical case with clear anatomical eligibility criteria, explicit use of cadaveric landmark data, and confirmed outcomes closes this gap and provides meaningful proof-of-concept, particularly for a technique that remains underutilized in resource-limited settings.

Novelty and Contribution

To the best of our knowledge, this represents one of the first Vietnamese cadaveric studies to systematically investigate the endoscopic transoral anatomy of the PPS from an inside-out perspective, providing quantitative distance measurements to the ICA from two clinically relevant landmarks. The integrated cadaveric-to-clinical design, in which the clinical case directly validates the cadaveric protocol, adds translational significance that purely descriptive anatomical studies cannot provide.

CONCLUSIONS

The ETA provides safe, direct access to the PPS through a reproducible, layer-by-layer anatomical corridor. Systematic inside-out dissection, with the pterygoid hamulus and stylopharyngeus muscle serving as key landmarks, enables reliable identification and protection of the ICA. The mean ICA distances from the pterygoid hamulus (26.75 mm) and pharyngeal mucosal surface (22.95 mm) provide quantitative reference values to guide intraoperative decision-making. The single clinical case confirms the direct applicability of these cadaveric findings and demonstrates the safety and feasibility of ETA for benign prestyloid PPS tumors. The integrated cadaveric-to-clinical design provides a translational framework supporting the standardization and broader adoption of ETA in modern head and neck surgery.

ACKNOWLEDGMENTS

The authors acknowledge the generous gift of the human cadaveric specimens used in this study. Donors and their families are recognized for their contribution to anatomical science and medical education (Iwanaga *et al*., 2021).

Conflict of interest. The authors declare that they have no conflict of interest.

TRAN, T. V.; LE, Q. T. & LAM, H. T. Abordaje endoscópico transoral al espacio parafaríngeo: estudio anatómico en cadáveres con validación mediante un caso clínico único. *Int. J. Morphol., 44(4)*:1500-1508, 2026.

RESUMEN: El espacio parafaríngeo (EPF) es un espacio cervical profundo cuya estrecha relación con la arteria carótida interna (ACI) y los nervios craneales inferiores hace que la cirugía en esta zona sea técnicamente exigente. El abordaje endoscópico transoral (AET) ofrece una alternativa mínimamente invasiva a las vías abiertas clásicas; sin embargo, siguen siendo escasas las descripciones cuantitativas sistemáticas de la anatomía visible desde una perspectiva interna a través de este corredor. El objetivo de este estudio fue: (1) describir la anatomía por planos del EPF tal como se observa durante la disección endoscópica trans oral en cadáveres frescos, midiendo la distancia a la ACI desde dos puntos de referencia clínicamente relevantes; y (2) validar la aplicabilidad clínica de estos hallazgos cadavéricos mediante un caso clínico único. Se realizó una disección endoscópica transoral en 10 cadáveres adultos frescos (20 lados) utilizando endoscopios rígidos de 0° y 30°, tras la inyección de contraste coloreado en la arteria carótida. Se registraron dos mediciones bilaterales con una precisión de 1 mm la distancia entre el gancho del proceso pterigoides y la ACI (PTH-ACI) y la distancia entre la mucosa faríngea y la ACI (Mucosa-ACI). Posteriormente, se sometió a AET a un paciente con un tumor en el compartimento prestiloideo del EPF que cumplía con los criterios anatómicos definidos en el estudio cadavérico. La disección secuencial permitió identificar sistemáticamente la mucosa faríngea, el músculo constrictor superior de la faringe, el compartimento graso prestiloideo, los músculos estilogloso y estilofaríngeo, el diafragma estilodeo y el ligamento estilohioideo antes de alcanzar la ACI. La distancia media PTH-ACI fue de 26,36 ± 2,94 mm (lado izquierdo) y 27,15 ± 5,11 mm (lado derecho); La media de la distancia mucosa-ACI fue de 22,85 ± 2,79 mm (izquierda) y 23,04 ± 2,42 mm (derecha). No se detectó ninguna asimetría significativa entre los lados izquierdo y derecho ($p > 0,05$). En el caso clínico, el tiempo quirúrgico fue de 45 minutos y la pérdida hemática inferior a 50 ml, sin complicaciones intraoperatorias; el estudio histopatológico confirmó un adenoma pleomórfico, sin recidiva a los seis meses. El estudio en cadáveres define un corredor anatómico estratificado y reproducible para el abordaje transoral endoscópico (ETA), identificando el gancho del proceso pterigoides y el músculo estilofaríngeo como referencias anatómicas de seguridad clave. El caso clínico confirma la traslación directa de los hallazgos cadavéricos a la práctica quirúrgica, respaldando la seguridad y viabilidad del ETA para tumores benignos del espacio parafaríngeo (EPF) preestiloideo de tamaño pequeño a mediano.

PALABRAS CLAVE: Espacio parafaríngeo; Abordaje transoral endoscópico; Anatomía quirúrgica; Estudio en cadáveres; Adenoma pleomórfico.

REFERENCES

Borello, A.; Castelli, M.; Riva, G. & Pecorari, G. Trans-oral removal of a large pleomorphic adenoma of the deep parotid lobe. *Indian J. Surg., 86*:629-31, 2024.

Boyce, B. J.; Curry, J. M.; Luginbuhl, A. & Cognetti, D. M. Transoral robotic approach to parapharyngeal space tumors: case series and technical limitations. *Laryngoscope, 126(8)*:1776-82, 2016.

Chan, J. Y. W.; Li, R. J.; Lim, M.; Hinojosa, A. Q. & Boahene, K. D. Endoscopic transvestibular paramandibular exploration of the infratemporal fossa and parapharyngeal space: a minimally invasive approach to the middle cranial base. *Laryngoscope, 121(10)*:2075-80, 2011.

Curtin, H. D. Separation of the masticator space from the parapharyngeal space. *Radiology, 163(1)*:195-204, 1987.

Dallan, I.; Seccia, V.; Muscatello, L.; Lenzi, R.; Castelnuovo, P.; Bignami, M.; Montevecchi, F.; Tschabitscher, M. & Vicini, C. Transoral endoscopic anatomy of the parapharyngeal space: a step-by-step logical approach with surgical considerations. *Head Neck, 33(4)*:557-61, 2011.

Gun, R.; Durmus, K.; Kucur, C.; Carrau, R. L. & Ozer, E. Transoral surgical anatomy and clinical considerations of lateral oropharyngeal wall, parapharyngeal space, and tongue base. *Otolaryngol. Head Neck Surg., 154(3)*:480-5, 2016.

Iwanaga, J.; Singh, V.; Ohtsuka, A.; Hwang, Y.; Kim, H. J.; Morys´, J.; Ravi, K. S.; Ribatti, D.; Trainor, P. A.; Sañudo, J. R.; Apaydin, N.; S¸engül, G.; Albertine, K. H.; Walocha, J. A.; Loukas, M.; Duparc, F.; Paulsen, F.; Del Sol, M.; Adds, P.; Hegazy, A. & Tubbs, R. S. Acknowledging the use of human cadaveric tissues in research papers: recommendations from anatomical journal editors. *Clin. Anat., 34(1)*:2-4, 2021.

Laccourreye, O.; Orosco, R. K.; Rubin, F. & Holsinger, F. C. Styloglossus muscle: a critical landmark in head and neck oncology. Eur. Ann. Otorhinolaryngol. *Head Neck Dis., 135(6)*:421-5, 2018.

Li, L.; London Jr., N. R.; Gao, Y.; Carrau, R. L. & Chen, X. Endoscopic transoral approach for resection of retrostyloid parapharyngeal space tumors: Retrospective analysis of 16 patients. *Head Neck, 42(12)*: 3531-7, 2020.

Li, L.; Gao, Y.; London Jr., N. R.; Kou, X.; Wang, W.; Xu, H. & Chen, X. Peri-operative complications following endoscopic-assisted transoral resection of parapharyngeal space tumors: retrospective analysis of 100 patients. *Eur. Arch. Otorhinolaryngol., 282*:2581-7, 2025.

Lombardi, D.; Ferrari, M.; Paderno, A.; Taboni, S.; Rampinelli, V.; Barbara, F.; Schreiber, A.; Mattavelli, D.; Tomasoni, M. & Farina, D. *et al*. Selection of the surgical approach for lesions with parapharyngeal space involvement: A single-center experience on 153 cases. *Oral Oncol., 109*:104872, 2020.

Olsen, K. D. Tumors and surgery of the parapharyngeal space. *Laryngoscope, 104(5 Pt. 2 Suppl. 63)*:1-28, 1994.

Paderno, A.; Piazza, C. & Nicolai, P. Recent advances in surgical management of parapharyngeal space tumors. *Curr. Opin. Otolaryngol. Head Neck Surg., 23(2)*:83-90, 2015.

Riffat, F.; Dwivedi, R. C.; Palme, C.; Fish, B. & Jani, P. A systematic review of 1143 parapharyngeal space tumors reported over 20 years. *Oral Oncol., 50(5)*:421-30, 2014.

Riva, G.; Lorenzi, A.; Borello, A.; Albera, A.; Canale, A. & Pecorari, G. Transoral approach to parotid tumors: a review of the literature. *Curr. Oncol., 29(12)*:9416-27, 2022.

Sun, X.; Yan, B.; Truong, H. Q.; Borghei-Razavi, H.; Snyderman, C. H. & Fernandez-Miranda, J. C. A comparative analysis of endoscopic-assisted transoral and transnasal approaches to parapharyngeal space: a cadaveric study. *J. Neurol. Surg. B Skull Base, 79(3)*:229-40, 2018.

Corresponding author:
Huyen Tran Lam
Department of Otorhinolaryngology
School of Medicine
University of Medicine and Pharmacy
at Ho Chi Minh City (UMP)
217 Hong Bang Street
Cho Lon Ward
Ho Chi Minh City
VIETNAM

E-mail: bstranent@gmail.com

Corresponding author:
Quang Tuyen Le
Department of Anatomy
Pham Ngoc Thach University of Medicine
Ho Chi Minh City
VIETNAM

E-mail: tuyenlequangdr@pnt.edu.vn